JVI Journals.ASM.org

# Disulfide Bonds in Hepatitis C Virus Glycoprotein E1 Control the Assembly and Entry Functions of E2 Glycoprotein

**Ahmed Wahid,[a,b] François Helle,[c] Véronique Descamps,[c] Gilles Duverlie,[c] François Penin,[d] Jean Dubuisson[a]**

Center for Infection and Immunity of Lille (CIIL), INSERM U1019, CNRS UMR8204, Institut Pasteur de Lille, Université Lille Nord de France, Lille, France[a]; Department of Biochemistry, Faculty of Pharmacy, Minia, University, Minia, Egypt[b]; Laboratoire de Virologie EA4294, Centre Hospitalier Universitaire d'Amiens, Université de Picardie Jules Verne, Amiens, France[c]; Institut de Biologie et Chimie des Protéines, Bases Moléculaires et Structurales des Systèmes Infectieux, UMR-5086-CNRS, Université de Lyon, Lyon, France[d]

**Class II membrane fusion proteins have been described in viruses in which the envelope proteins are derived from a precursor polyprotein containing two transmembrane glycoproteins arranged in tandem. Although the second protein, which carries the membrane fusion function, is in general well characterized, the companion protein, which is a protein chaperone for the folding of the fusion protein, is less well characterized for some viruses, like hepatitis C virus (HCV). To investigate the role of the class II companion glycoprotein E1 of HCV, we chose to target conserved cysteine residues in the protein, and we systematically mutated them in a full-length infectious HCV clone by reverse genetics. All the mutants were infectious, albeit with lower titers than the wild-type virus. The reduced infectivity was in part due to a decrease in viral assembly, as revealed by measurement of intracellular infectivity and by quantification of core protein released from cells transfected with mutant genomes. Analyses of mutated proteins did not show any major defect in folding. However, the mutations reduced virus stability, and they could also affect the density of infectious viral particles. Mutant viruses also showed a defect in cell-to-cell transmission. Finally, our data indicate that HCV glycoprotein E1 can also affect the fusion protein E2 by modulating its recognition by the cellular coreceptor CD81. Therefore, in the context of HCV, our data identify an additional function of a class II companion protein as a molecule that can control the binding capacity of the fusion protein.**

Hepatitis C virus (HCV) infection is a major public health problem, with as many as 160 million people infected worldwide (1). The virus has a high propensity to establish a persistent infection in the human liver. HCV primarily infects human hepatocytes, which over time leads to chronic inflammation, progressive fibrosis, and development of hepatocellular carcinoma. Recent improvements in the standard of care therapy, now a combination of pegylated interferon, ribavirin, and an inhibitor of HCV protease NS3/4A, have raised the hope that HCV infection can be managed efficiently in countries with adequate medical infrastructure. However, further improvements in antiviral therapy are still needed, and the development of a prophylactic vaccine would be of high value in countries where prevalence is elevated.

HCV is a small enveloped virus classified in the genus *Hepacivirus* within the family *Flaviviridae*. Its positive-strand RNA genome encodes a single polyprotein that is processed by cellular and viral proteases into 10 mature proteins (2). Cleavage of the viral polyprotein by a cellular signal peptidase gives rise to the envelope glycoproteins E1 and E2, which play a crucial role in HCV entry into host cells (reviewed in reference 3). Three classes of viral membrane fusion proteins have been described so far (4), and HCV has been proposed to contain a class II fusion protein (5). Class II proteins have been described in viruses in which the envelope proteins are derived from a precursor polyprotein containing two transmembrane glycoproteins arranged in tandem (4). The first glycoprotein acts as a companion chaperone for the folding of the second one, which carries the membrane fusion function. As for other class II viruses, HCV envelope glycoproteins assemble as a noncovalent heterodimer within the endoplasmic reticulum (ER) (6). Within the E1E2 complex, E2 is currently the better characterized subunit. Indeed, the glycoprotein is considered the major target of neutralizing antibodies, and it is also the receptor-binding protein, which has been shown to interact with CD81 tetraspanin and scavenger receptor BI (SRB1), two HCV coreceptors (reviewed in reference 7). Finally, E2 has also been proposed to be an HCV fusion protein (5). In contrast, the role of the E1 companion subunit in HCV remains poorly defined. However, E1 has also been proposed to be involved in the fusion process (8, 9, 10).

The structure of HCV envelope glycoproteins is stabilized by intramolecular disulfide bridges (5, 11, 12). Proteins that traverse the secretory pathway, like HCV envelope glycoproteins, acquire disulfide bonds while they fold in the ER (13). Disulfide bonds are considered essential for folding stability and/or for the structure and function of mature proteins. This explains why the disulfide-bonded structure of proteins is usually conserved across species and within protein families. Viral glycoproteins involved in virus entry into host cells need to change conformation at different steps of the viral life cycle (14). For this reason, disulfide bonds within these proteins are even more important to keep them functional. For instance, all 18 conserved cysteine residues of HCV glycoprotein E2 are absolutely required for the production of infectious virus (15). Similarly, 8 of the 10 strictly conserved disulfide bonds are essential for the function of HIV-1 envelope glycoprotein (16). Although disulfide bonds have been shown to be

**Received** 26 September 2012 **Accepted** 9 November 2012
**Published ahead of print** 21 November 2012
Address correspondence to Jean Dubuisson, jean.dubuisson@ibl.fr.

doi:10.1128/JVI.02659-12

essential for the functions of the E2 subunit, nothing is known about the role of cysteine residues in its E1 partner. The glycoprotein possesses eight cysteine residues within its ectodomain, which are fully conserved across the seven genotypes. The disulfide arrangement of these eight cysteines has not yet been determined. This is mainly due to difficulties in expressing E1 alone in sufficient quantity for biochemical characterization (17).

Here, we investigated the role of the class II companion glycoprotein E1 of HCV in the context of the viral life cycle. We chose to target conserved cysteine residues in the protein, and we systematically mutated them in the context of a full-length infectious HCV clone by reverse genetics. The mutations were analyzed for their effects on HCV glycoprotein folding, on viral particle assembly/release, and on virus entry. All the mutants were infectious, albeit with some level of attenuation, which is in part due to alteration in virus assembly. The mutations reduced virus stability, and they could also affect the density of infectious viral particles. These mutants also showed some defect in cell-to-cell transmission. Finally, all these mutations induced better accessibility of the CD81 binding site on E2 glycoprotein present on the virion, indicating that E1 controls the structure and function of E2 on the surface of the HCV particle.

## MATERIALS AND METHODS

**Sequence analyses and structure predictions.** Sequence analyses were performed using the website tools of the European HCV database (euHCVdb) (18) and network protein sequence analysis (NPSA) (19), available at the Institut de Biologie et Chimie des Protéines. Multiple-sequence alignments and amino acid conservation analysis were carried out with the ClustalW program using default parameters (20). Various methods were combined for the prediction of membrane binding sequences as follows: DAS (21), HMMTOP (22), TMpred (23), TMHMM (24), Top-Pred (25), and SOSUI (26).

**Cell culture.** The cell-based fluorescent-reporter system, which allows sensitive distinction of individual HCV-infected cells of the Huh7-RFP-NLS-IPS hepatoma cell line, was generated as described previously (27). This cell line and the parental Huh-7 hepatoma cell line (27, 28) were grown in Dulbecco's modified essential medium (DMEM) (Invitrogen) supplemented with 10% fetal calf serum.

**Antibodies.** Anti-HCV monoclonal antibodies (MAbs) A4 (anti-E1) (29) and 3/11 (anti-E2; kindly provided by J. A. McKeating, University of Birmingham, Birmingham, United Kingdom [30]) were produced *in vitro* by using a MiniPerm apparatus (Heraeus) as recommended by the manufacturer. The anti-NS5A MAb 9E10 (31) and a polyclonal antibody were kindly provided by C. M. Rice (Rockefeller University, New York, NY) and M. Harris (University of Leeds, Leeds, United Kingdom), respectively. Anti-ApoE antibody was from EMD Millipore. Secondary antibodies used for immunofluorescence were purchased from Invitrogen.

**Mutagenesis and production of viruses.** The virus used in this study was based on the JFH1 isolate (genotype 2a; GenBank accession number AB237837) (32), kindly provided by T. Wakita (National Institute of Infectious Diseases, Tokyo, Japan). Mutations were introduced in a modified version of the plasmid carrying the full-length JFH-1 genome. This virus contains mutations at the C terminus of the core protein leading to amino acid changes F172C and P173S, which have been shown to increase viral titers (33). Furthermore, the N-terminal E1 sequence encoding residues 196TSSSYMVTNDC has been modified to reconstitute the A4 epitope (SSGLYHVTNDC), as described previously (34). Cysteine mutants were generated by site-directed mutagenesis with the Quik-change system according to the manufacturer's instructions (Invitrogen, Stratagene, La Jolla, CA). Cysteine residues were replaced by alanines. The restriction enzyme XbaI was used to linearize plasmids encoding viral RNAs. The linearized plasmids were then treated with mung bean nuclease (New England BioLabs) with the aim of obtaining blunt-ended DNA. For *in vitro* transcription, 1 μg of linearized DNA was transcribed using the Megascript kit according to the manufacturer's protocol (Ambion). The *in vitro* transcription reaction mixture was set up and incubated at 37°C for 4 h, and transcripts were precipitated by the addition of equal volumes of LiCl and nuclease-free water. The mixture was chilled at −20°C for 30 min and then centrifuged at 4°C for 15 min at 14,000 × *g*. The supernatants were then removed, and the RNA pellets were washed with 70% ethanol and resuspended in RNase-free water. The nonreplicative control of the HCV genome (GND) contained a GND mutation in the NS5B active site, as previously reported (32). The assembly-deficient control of HCV (ΔE1E2) containing an in-frame deletion introduced into the E1E2 regions of constructs was as previously described (32).

**Immunofluorescence.** Huh-7 cells electroporated with the wild type (WT) and E1 mutants were grown on 12-mm coverslips. After 48 h, the cells were washed twice with 1× phosphate-buffered saline (PBS) and then fixed with cold methanol (100%) for 5 min or 3% paraformaldehyde (PFA) for 20 min. The PFA and methanol were removed by washing the cells twice with 1× PBS. The cells were then blocked with 10% goat or horse serum for at least 10 min, followed by washing with 1× PBS. The primary anti-NS5A antibody (31) was diluted in goat serum/horse serum, and the coverslips were incubated with antibodies at room temperature for 25 min. The cells were washed 3 times in PBS and incubated for 5 min between washes. The secondary antibody was diluted in goat serum/horse serum (1:800), and coverslips were incubated with the peroxidase-conjugated antibody for 20 min. The cells were washed again with 1× PBS. Nuclei were stained with DAPI (4′,6-diamidino-2-phenylindole). The coverslips were mounted on glass slides using 30 μl of mounting medium (Mowiol 4-88; Calbiochem). The slides were finally observed under a fluorescence microscope.

**Fifty percent tissue culture infective dose ($TCID_{50}$) infectivity assays.** Viruses were harvested at different times following electroporation as described previously (33), and the supernatants were used to infect naive Huh-7 cells for 48 h. The infected cells were then fixed with ice-cold methanol (100%) and immunostained with anti-NS5A antibody using MAb 9E10 or sheep anti-NS5A antiserum.

**Intracellular infectivity assay.** Supernatants containing extracellular virus were harvested 72 h after electroporation, and cell debris was removed by centrifugation for 5 min at 10,000 × *g*. The cells were washed with PBS, harvested by treatment with trypsin, and pelleted at 100 × *g* for 5 min. The cell pellets were resuspended in complete medium and mechanically lysed in a Dounce homogenizer (30 strokes). The cell lysates were clarified by centrifugation at 10,000 × *g* for 5 min. Supernatants containing extracellular or intracellular virus were collected and used for infection of naïve cells.

**Stability assays.** Viruses were harvested 72 h following electroporation (33). Virus in culture medium was then dispensed in 100-μl aliquots in 1.5-ml microcentrifuge tubes and then incubated at 37°C. At designated time points, aliquots were removed and subjected to $TCID_{50}$ infectivity assays for virus titration.

**Equilibrium density gradient analysis.** Viruses were harvested 72 h following electroporation as described previously (33). Approximately 55 ml of virus supernatants was precipitated using polyethylene glycol (PEG) 6000 to a final concentration of 8%. The mixture was shaken for 1 h on ice, centrifuged at 8,000 rpm (Beckman JA10 rotor) for 25 min, and then resuspended with 1 ml sterile PBS. Before loading, the virus was once again centrifuged for 5 min at 5,000 × *g* to remove insoluble materials. Continuous 10 to 50% iodixanol gradients were formed by equal-volume steps of 10 to 50% iodixanol solutions in sterile PBS (at 5% increments) and incubation at 4°C for 4 h. The concentrated virus was then loaded onto the top of the gradient. The gradients were spun for 16 h at 36,000 rpm in an SW41 rotor (Beckman) and fractionated from the top. Following centrifugation, 11 fractions of 1 ml each were analyzed for their infectivity (100-μl sample). Fraction densities were also determined.

**HCV core quantification.** HCV core was quantified by a fully automated chemiluminescent microparticle immunoassay according to the manufacturer's instructions (Architect HCVAg; Abbott, Germany) (35, 36). Electroporated Huh-7 cells were lysed in PBS lysis buffer (1% Triton X-100, 20 mM *N*-ethylmaleimide [NEM], 2 mM EDTA, protease inhibitor cocktail; Roche). The lysates were then cleared by centrifugation for 15 min at 14,000 × *g*. The supernatants were also harvested to obtain the extracellular core protein. Intracellular, as well as extracellular, core quantities were then determined.

**Western blotting.** Cells were lysed in 1× PBS lysis buffer (1% Triton 100-X, 20 mM NEM, 2 mM EDTA, protease inhibitor cocktail; Roche). The cell lysates were then precleared by centrifugation at 14,000 × *g* for 15 min at 4°C. Protein samples were heated for 7 min at 70°C in Laemmli sample buffer. Beta-mercaptoethanol was added to the Laemmli buffer only at a working concentration of 100 mM for reducing SDS-PAGE conditions. Following separation with SDS-PAGE, the proteins were transferred onto nitrocellulose membranes (Hybond-ECL; Amersham) using a transblot apparatus and revealed with specific antibodies. The E1 and E2 glycoproteins were detected with MAb A4, since its epitope has been reconstructed into the JFH1 genome, and rat MAb 3/11, which recognizes a conserved epitope in E2, respectively. Following incubation with primary antibodies, the membranes were incubated with the corresponding peroxidase-conjugated anti-species antibodies at 1/5,000 (anti-rat [Jackson] and antirabbit [Amersham]) or 1/10,000 (anti-mouse [Dako]) dilution. E1 and E2 proteins were revealed by enhanced chemiluminescence (ECL) (Amersham) as recommended by the manufacturer.

**CD81 pulldown assay.** Cells were lysed in 1× PBS lysis buffer (1% Triton X-100, 20 mM NEM, 2 mM EDTA, protease inhibitor cocktail; Roche). The cell lysates were then cleared by centrifugation at 14,000 × *g* for 15 min at 4°C. Glutathione-Sepharose beads (glutathione-Sepharose 4B; Amersham Bioscience) (37) were washed twice with cold PBS to remove the storage buffer. For each cell lysate sample, 50 μl of glutathione beads was incubated with 10 μg of human CD81 (hCD81)–large extracellular loop (LEL)–glutathione *S*-transferase (GST) recombinant protein in 1 ml cold PBS for 2 h at 4°C. Following incubation, the glutathione-Sepharose beads were washed with cold PBS. Cell lysate samples containing E1E2 proteins were then incubated with CD81 complexed with glutathione beads overnight at 4°C. The following day, the beads were washed five times with cold PBS and 0.1% Triton X-100. Finally, the beads were resuspended in 30 μl of reducing Laemmli buffer (200 mM Tris-HCl, pH 6.7, 0.5% SDS, 10% glycerol) containing 100 mM beta-mercaptoethanol for reducing conditions. Samples were boiled and loaded onto 12% SDS-PAGE, followed by Western blotting to reveal the target protein.

**CD81 inhibition assays.** Ten micrograms of HCV RNA was electroporated into Huh-7 cells as described previously (33). Viruses were preincubated with human or murine CD81-LEL for 2 h at 37°C. The viruses were then put in contact with Huh-7 cells. After 3 h of contact, the cells were further incubated for 48 to 72 h with complete medium. The cells were immunolabeled, and the infected cells were counted. The concentrations resulting in 50% inhibition were then determined.

**Analysis of sensitivity to pH treatment.** Huh-7.5 cells were treated with bafilomycin A1 (25 nM) for 1 h at 37°C and then infected with WT JFH-1 or mutant viruses in the presence of bafilomycin A1 for 2 h at 4°C. After 2 h, the cells were sequentially washed with cold phosphate-buffered saline and with citric acid buffer, pH 7 or pH 5, for 5 min at 37°C. Infected cells were further incubated in DMEM containing 10% fetal bovine serum (FBS) in the presence of bafilomycin A1 for 48 h.

**Direct cell-to-cell transmission assays.** HCV cell-to-cell transmission was measured as described previously (38). Briefly, Huh-7 cells (60,000) were seeded in 24-well plates; the next day, 1,000 infected Huh7-RFP-NLS-IPS cells were cocultured in each well. The cultures were treated with 10 μl/ml of anti-E2 MAb 3/11 and fixed with 3% PFA at 72 h after culture. HCV-infected acceptor cells were then visualized with the anti-NS5A MAb 9E10 in combination with Alexa Fluor 488-conjugated donkey anti-sheep antibody.

## RESULTS

**Conservation of cysteine residues in HCV glycoprotein E1.** Kinetic studies in cell culture indicate that HCV glycoprotein E1 slowly acquires intramolecular disulfide bonds in the presence of HCV glycoprotein E2 (11, 39, 40, 41). E1 possesses eight cysteine residues within its ectodomain at positions 207, 226, 229, 238, 272, 281, 304, and 306, which are highly conserved in all genotypes (Fig. 1, highlighted in magenta). Indeed, examination of 2,230 full-length E1 sequences of any genotype revealed only 36 sequences showing a single cysteine mutation. The frequencies of mutation are comparable at all cysteine positions and correspond to a single codon base mutation. The exceptional conservation of the cysteine residues among HCV genotypes argues for a major role of these amino acids in the functions of E1 protein. It is expected that four disulfide bonds could be formed to stabilize the folding of E1, but due to difficulties in expressing E1 alone, these disulfide bonds have not yet been determined. Cys 207, 304, and 306 are all located in rather hydrophilic coil regions (highlighted in yellow in Fig. 1), while the others belong to more hydrophobic regions (highlighted in gray), with some of them predicted to be involved in stable secondary structures (Cys 229, 238, and 272 [Second. cons. in Fig. 1]). It is worth noting that Cys 226 and 229 are separated by 2 amino acids, as in a protein disulfide isomerase (PDI) motif. Finally, Cys 272 and 281 belong to an enigmatic predicted membrane binding segment (MBS) (Fig. 1) postulated to contain a fusion peptide-like motif (9) and identified as playing a role in the membrane fusion process (10). A synthetic peptide spanning residues 268 to 298 encompassing the putative E1 fusion peptide-like motif has been experimentally shown to mediate high levels of both hemifusion and complete fusion (46).

**Effects of E1 cysteine mutations on HCV infectivity.** Since disulfide bonds have not been determined in E1, we could not precisely disrupt them by double mutation of the involved cysteine residues. We therefore chose to disrupt the cysteine residues individually, which, if they were involved in a disulfide bond, would also disrupt cysteine-cysteine interaction. To determine the roles of the individual cysteine residues of E1 in different steps of the HCV life cycle, we produced a complete series of mutants in which cysteine residues were individually replaced by alanine residues. In addition, to determine the potential role of the PDI-like motif in E1, we also constructed a double mutant in the motif (C226A-C229A). To characterize these mutants, we first measured the effects of the mutations on the production of infectious virus. The infectivities of the generated mutant viruses were determined. Supernatants of cells electroporated with mutant RNAs were collected after 48, 72, and 96 h. A viral genome carrying a large in-frame deletion in the E1E2 coding region (ΔE1E2) known to inactivate release of viral particles and a genome containing an inactive mutation in NS5B polymerase (GND) were used as negative controls for virus assembly and replication, respectively (32).

As shown in Fig. 2, all the mutants showed a decrease in infectivity. Indeed, compared to the WT virus, the cysteine mutants showed average $\log_{10}$ reductions of 2.1, 1.7, and 1.6 at 48, 72, and 96 h postelectroporation, respectively. It is worth noting that the C226A-C229A double mutant did not show further decrease in infectivity compared to the single mutations, suggesting that the PDI-like motif in E1 is not essential for the HCV life cycle. The most severe difference in infectivity between WT and E1 mutants was observed at 48 h postelectroporation for the C207A, C226A,

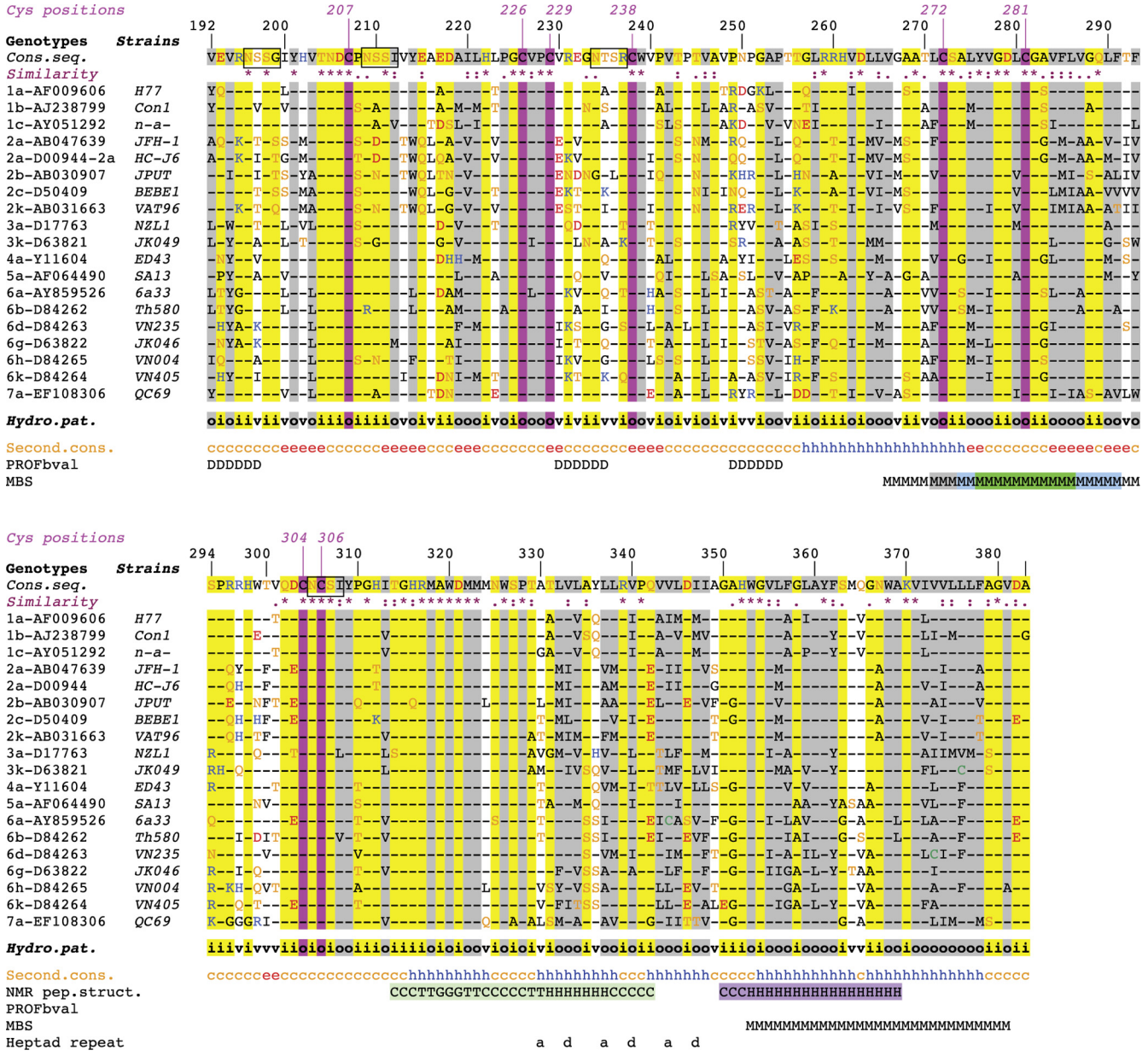


**FIG 1** Sequence variability, cysteine residue conservation, and structural elements of the E1 glycoprotein. Shown are multiple alignments of E1 sequences from representative HCV strains of confirmed genotypes (http://euhcvdb.ibcp.fr/euHCVdb/) (18). Genotype and accession number (in the Genotypes column) and strain are indicated for each sequence. Amino acids are numbered with respect to the polyprotein of HCV strain H77, used as a reference (top row) (42). The positions of conserved cysteine residues are indicated in magenta (top row). The consensus sequence (Cons. seq.) was deduced from the ClustalW multiple alignment of the indicated E1 sequences (20). The boxes indicate the N-glycosylation sites common to all genotypes. To highlight the amino acid variability at each position, amino acids identical to the consensus sequence are indicated by dashes. The degree of amino acid physicochemical conservation at each position can be inferred by the similarity index according to ClustalW convention (asterisk, invariant; colon, highly similar; dot, similar) (20) and the consensus hydropathic pattern (Hydro. pat.): o, hydrophobic position (Phe, Ile, Trp, Tyr, Leu, Val, Met, Pro, or Cys); n, neutral position (Gly, Ala, Thr, or Ser); i, hydrophilic position (Lys, Gln, Asn, His, Glu, Asp, or Arg); v, variable position (i.e., when both hydrophobic and hydrophilic residues are observed at a given position). To highlight the variable sequence positions in E1, conserved hydrophilic and hydrophobic positions are highlighted in yellow and gray, respectively. The fully conserved cysteine positions are highlighted in magenta. Polar and positively and negatively charged residues are color coded in orange, blue, and red, respectively. Cysteine residues are in green, and all other residues are in black. For Second. cons. (bottom row), consensus secondary-structure predictions of E1 from representative HCV strains are indicated as helical (h; blue), extended (e; red), or undetermined (coil [c]; orange). Predictions were made by using the Web-based algorithms SOPM, HNN, DSC, GOR IV, PHD, Predator, and SIMPA96, available at the NPSA website (http://npsa-pbil.ibcp.fr; reference 19 and references therein). NMR pep. Struct. (bottom row) reports the conformation of residues observed in the corresponding synthetic peptides analyzed by nuclear magnetic resonance (NMR). E1 peptide 314 to 342 are highlighted in green (45) (Protein Data Bank [PDB] entry 2KNU), and E1 peptide 350 to 369 are highlighted in violet (43) (PDB entry 1EMZ). Residue conformations are indicated as helical (H), 3/10 helix (G), turn (T), or undetermined (C). Flexible residue regions (indicated as "D" in the bottom row) were predicted using PROFbval software (44). MBS, consensus membrane binding segments predicted by the available Web-based algorithms DAS, HMMTOP, TMpred, TMHMM, TopPred, and SOSUI. Heptad repeat, weakly conserved heptad repeat region (9).

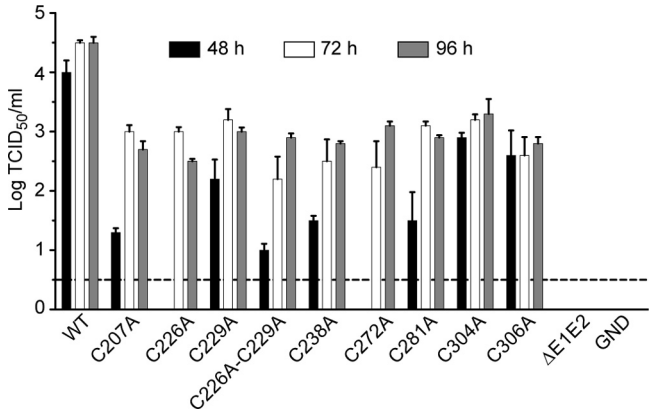


**FIG 2** Effects of E1 cysteine mutations on HCV infectivity. Huh-7 cells were electroporated with viral RNA transcribed from different JFH1-derived mutants. At 48, 72, and 96 h postelectroporation, the infectivity of the supernatants was determined by titration. The error bars indicate standard errors of the mean (SEM) from at least three independent experiments. The dashed line indicates the detection limit of the assay.

C229A, C226A-C229A, C238A, C272A, and C281A mutants (Fig. 2), indicating some delay in the production and/or secretion of infectious particles. The most dramatic effect was observed for the C226A and C272A mutants, for which no infectivity was observed at 48 h postelectroporation. However, the levels of infectivity of these two mutants were similar to those of the other mutants at 72 and 96 h postelectroporation. It is also worth noting that the C304A and C306A viruses were the least affected mutants, since they showed the highest infectivity at 48 h postelectroporation.

It has been shown previously that significant amounts of infectious virions are present inside infected cells and that they can be recovered by several freeze-thaw cycles (47). Thus, in order to study the effects of cysteine mutations on the secretion of viral particles, we tried to investigate the intracellular infectivity of the mutated viruses. To our surprise, the infectivity of the mutated viruses was totally lost after a single freeze-thaw cycle, and viral stocks kept at −80°C lost their ability to infect naive Huh-7 cells. Therefore, infectivity could be recovered only upon using fresh unfrozen stocks of virus. This observation suggests that disulfide bonds in E1 stabilize the structures of the envelope proteins associated with HCV particles.

Altogether, our results indicate that mutations of cysteine residues in E1 affect the viral titers of released particles. However, these residues are not essential for viral infectivity, since in contrast to E2 mutants (12), none of the E1 mutants were dead. Rather, they contribute to the stability of the structures of HCV envelope proteins associated with HCV particles.

**Mutations of cysteine residues in E1 reduce HCV particle stability.** Since we noticed that the infectivity of the mutants was lost after a single freeze-thaw cycle, we further investigated the stability of these viruses at 37°C. Virus stocks were kept at 37°C, and at designated time points (0, 6, 12, 24, 48, and 96 h), aliquots were removed and infectivity was measured. For each mutant, the half-life ($t_{1/2}$) was calculated after fitting the data to the most appropriate linear regression model ($R^2 = 0.99$) (Table 1). As shown in Fig. 3, all the mutants were found to be less stable than the WT. We noticed that infectivity decreased more sharply between 12 and 24 h, and it was completely lost at day 4.

**Mutations of cysteine residues in E1 affect the assembly of the HCV particle.** Although HCV particle stability is affected by cysteine mutations, this does not by itself explain the low infectious titers recovered after electroporation (Fig. 2 and 3). We therefore anticipated that the reduced infectivity could rather be due to a defect in viral secretion or to the release of noninfectious particles. To study the effects of our cysteine mutations on the secretion of viral particles, we compared the amounts of intracellular and extracellular infectious viruses produced upon transfection of Huh-7 cells with our mutants. However, since we could not freeze our mutants, we mechanically lysed infected cells with a Dounce homogenizer to harvest intracellular virus. We then compared the amounts of intracellular and extracellular infectious viruses produced upon transfection of Huh-7 cells with our mutants. As shown in Fig. 4A, there was no increase in intracellular infectivity for the mutants, indicating that the mutations had no effect on the efficiency of virion release but rather affected viral particle assembly or specific infectivity.

To distinguish between these two possibilities, we monitored the release of HCV core into the supernatant of electroporated cells using a fully automated chemiluminescent microparticle immunoassay as described previously (35, 36). In parallel, core protein was also quantified in cell lysates to verify the potential effects of the mutations on genomic replication. As shown in Fig. 4B, for all the cysteine mutants, the level of core protein expression was similar to that of the WT, indicating that the mutations did not affect HCV genomic replication. In contrast, the quantity of core protein in supernatants decreased drastically compared to the WT (Fig. 4C), paralleling the decrease in infectivity (Fig. 2). Together with the observation that there is no effect on virus release, these data indicate that mutations of cysteine residues in E1 affect the assembly of HCV particles. However, specific infectivities remained lower for the mutants after normalizing them to the amount of secreted core protein (Fig. 4D), indicating that the entry functions of HCV particles were also reduced when cysteine residues were mutated in E1. This could suggest that the fusion properties of HCV envelope proteins are less optimal in the context of our mutations.

**Mutations of cysteine residues in E1 do not affect E1E2 heterodimerization.** Since HCV envelope glycoprotein subunits cooperate during their folding for the formation of E1E2 heterodimer (17, 39, 48), we wanted to determine whether our mutants affect the formation of the E1E2 heterodimer, which is the functional HCV glycoprotein unit in infected cells (6). We first

**TABLE 1** Half-lives of E1 cysteine mutants at 37°C

| Strain | Half-life (h) | SEM |
|---|---|---|
| WT | 25.6 | 3.06 |
| C207A | 11.3 | 2.74 |
| C226A | 12.7 | 2.79 |
| C229A | 12.3 | 3.21 |
| C226-229A | 12.7 | 2.79 |
| C238A | 11.8 | 3.83 |
| C272A | 13.8 | 2.83 |
| C281A | 11.5 | 3.29 |
| C304A | 13.3 | 3.66 |
| C306A | 13.3 | 2.74 |
| ΔE1E2 | 0 | 0 |
| GND | 0 | 0 |

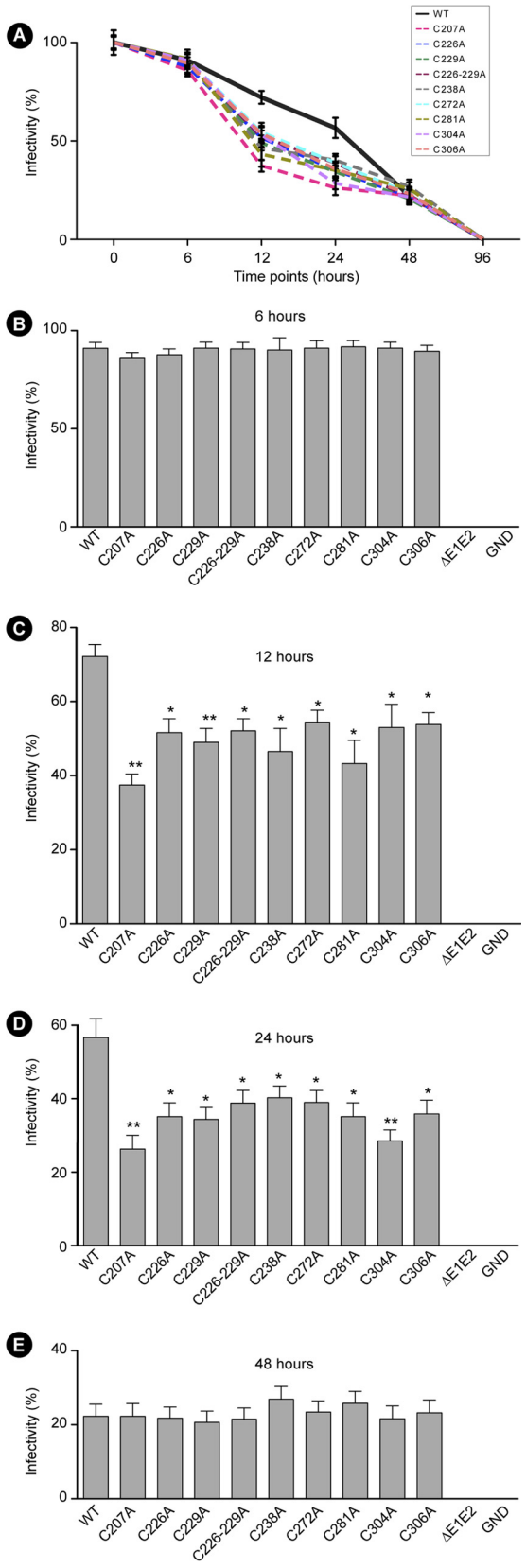


**FIG 3** Mutations of cysteine residues in E1 reduce HCV particle stability. (A) Virus from 72 postelectroporation cultures was dispensed in 100-μl aliquots in 1.5-ml microcentrifuge tubes and then incubated at 37°C. At designated time points (0, 6, 12, 48, and 96 h), aliquots were removed and then subjected to $TCID_{50}$ infectivity assays for virus titration. The data were fitted to the most appropriate linear regression model ($R^2 = 0.99$). The values are the combined data from two independent experiments; the error bars represent SEM. (B to E) Percentages of infection at 6 (B), 12 (C), 24 (D), and 48 (E) h. Differences were considered statistically significant if $P$ was $<0.05$.

analyzed the expression of HCV glycoproteins individually by SDS-PAGE under reducing and nonreducing conditions to determine whether the absence of a cysteine residue in E1 can lead to the formation of disulfide bond aggregates involving both E1 and E2. As expected, E1 and E2 proteins could be readily detected in cell lysates (Fig. 5). Furthermore, for all the mutants, the levels of expression of E1 and E2 were similar to those of the WT when analyzed under reducing conditions (Fig. 5A, Reducing). It must be noted that a second band migrating slightly faster was observed for the C306A mutant. Since this mutation is very close to an N-linked glycosylation site at position 305, it is likely that the mutation affects the glycosylation of the site and that the faster-migrating band of the C306A mutant might correspond to an E1 glycoform lacking this glycan. It is worth noting that the additional band detected in the upper part of the gel by the anti-E1 antibody might correspond to trimers of E1, as observed previously (6). This putative trimeric E1 band disappeared in the C272A and C281A mutants, suggesting a role for these two cysteine residues in stabilizing E1 homo-oligomers. Analyses of HCV envelope glycoproteins under nonreducing conditions did not show any increase in intermolecular disulfide bonds between HCV envelope glycoproteins (Fig. 5A, Non-Reducing), indicating that removal of cysteine residues in E1 does not lead to the formation of aggregates.

Although direct analyses of HCV envelope glycoproteins by Western blotting under reducing and nonreducing conditions did not show any major effect on the expression of HCV envelope glycoproteins, we could not exclude additional effects that cannot be discriminated by this type of analysis. To further analyze the effects of these mutations on HCV glycoprotein heterodimerization, we used the LEL of CD81, an HCV coreceptor (49), as a probe to determine the formation of properly folded E1E2 complexes in a pulldown assay. Indeed, the CD81-binding domain in E2 is conformation sensitive (50), and interaction of E1 with properly folded E2 protein is an indirect proof that the protein is properly folded (40). As shown in Fig. 5B, properly folded E1E2 complexes recognized by CD81 are formed for all the mutants at levels comparable to those of the WT. The only difference is in the C306A mutant, for which an additional band was observed. As discussed above, this band likely corresponds to a glycoform of E1 lacking a glycan at position 305. Together, these data indicate that mutations of cysteine residues in E1 do not affect E1E2 heterodimerization.

**E1 cysteine mutants do not overcome the cell entry blockade induced by bafilomycin at acidic pH.** After cell surface binding and virus internalization into clathrin-coated pits, HCV infection is mediated by conformational changes of the viral glycoprotein E1E2 complex, which are triggered by low pH (51, 52). However, in contrast to most pH-sensitive viruses, exposing HCV particles, directly after binding to permissive cells at 4°C, to a low-pH wash does not efficiently initiate infection. In contrast, chasing these particles for 1 h at 37°C increases their sensitivity to low pH, which

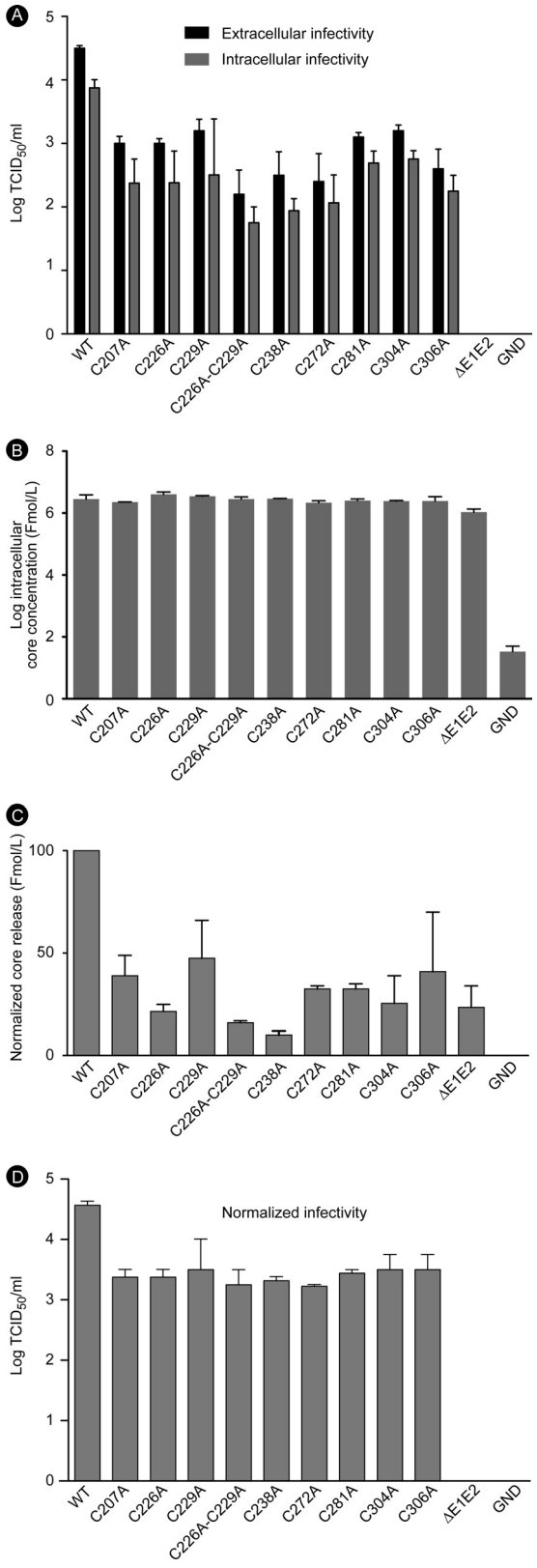


**FIG 4** Mutations of cysteine residues in E1 affect HCV assembly. (A) Effects of E1 cysteine mutations on infectious-virus secretion. Huh-7 cells were electroporated, and at 72 h posttransfection, the supernatants were collected. In parallel, virus-producing cells were washed and mechanically lysed. Extracellular and intracellular infectivities were determined by titration. (B and C) Mutations of cysteine residues in E1 affect the release of HCV core protein. Huh-7 cells were electroporated with viral RNA transcribed from different JFH1-derived mutants. At 72 h postelectroporation, the amount of intracellular core antigen was determined in cell lysates (B), as well as in supernatants (C). The amounts of core protein in cell supernatants were divided by the corresponding amounts in cell lysates and normalized to the WT value. (D) Infectivity of E1 mutants after normalization of the amount of virions released in the supernatant by measuring extracellular core protein. The error bars indicate SEM.

may indicate that HCV entry requires certain additional stimuli (52) that might involve the dissociation of inter- or intramolecular disulfide bonds, as suggested previously (6). We therefore wanted to test whether mutations of cysteine residues in E1 might reduce the dependence on additional stimuli for low-pH-induced fusion at the plasma membrane. To test this hypothesis, we compared the responsiveness of our mutants to low-pH treatment following the protocol described by Tscherne et al. (52). Infection via acidified endosomes was blocked throughout these experiments by treatment of target cells with bafilomycin A1, an inhibitor of vacuolar-type $H^+$-ATPase. This compound inhibits endosomal acidification and hence inhibits cell entry of the virus through the natural endosomal route. In our experiments, cells were infected with HCV E1 cysteine mutants at 4°C for 2 h, washed with acidic buffer, and further incubated at normal pH for 48 h. Compared to the WT, none of the mutants showed any increase in infectivity under these conditions (Fig. 6), indicating that cell-bound HCV mutants remain acid resistant and that, as for WT virus, they require an additional trigger for low-pH-induced infection.

**E1 cysteine mutants show a defect in direct cell-to-cell transmission.** Following infection of Huh-7 cells with HCV, progeny viruses can be transmitted to adjacent cells by cell-to-cell contacts, resulting in focal areas of spreading infection (53, 54). This mode of transmission is refractory to neutralization by anti-E2 antibodies (53). To determine the effects of E1 cysteine mutations on cell-to-cell spread, we cocultured naive Huh-7 cells with JFH1-infected Huh7-RFP-NLS-IPS cells. The latter cells are stably transduced to express a red fluorescent dye in the cytoplasm that translocates into the nucleus upon HCV infection (27). This approach allows us to easily discriminate between donor and acceptor cells, and it rules out the possibility that clusters of infected cells are derived from dividing donor cells rather than from spread of the virus. In these cocultures, cells were incubated with neutralizing MAb 3/11 to prevent cell-free infection (55). HCV acceptor cells were visualized via immunofluorescence microscopy, and the number of cells per focus was determined. As shown in Fig. 7, the mean number of cells per focus was very low for E1 cysteine mutants. Indeed, in the presence of MAb 3/11, on average, 68.9 acceptor cells were present per focus for the WT virus, whereas between 1 and 2 cells per focus were counted for the mutants. This low number of cells per focus could be due in part to a defect in particle secretion. However, higher numbers of cells per focus were observed for the mutants in the absence of antibodies (Fig. 7A), indicating some level of particle production. Indeed, in the absence of MAb 3/11, on average, between 7 and 12 cells per focus were counted for the mutants, whereas on average, a mean value of 108 acceptor cells were present per focus for the WT virus. Although a defect in virus assembly can impact cell-to-cell transmission, as well as cell-free infection, a stronger decrease in cell-to-

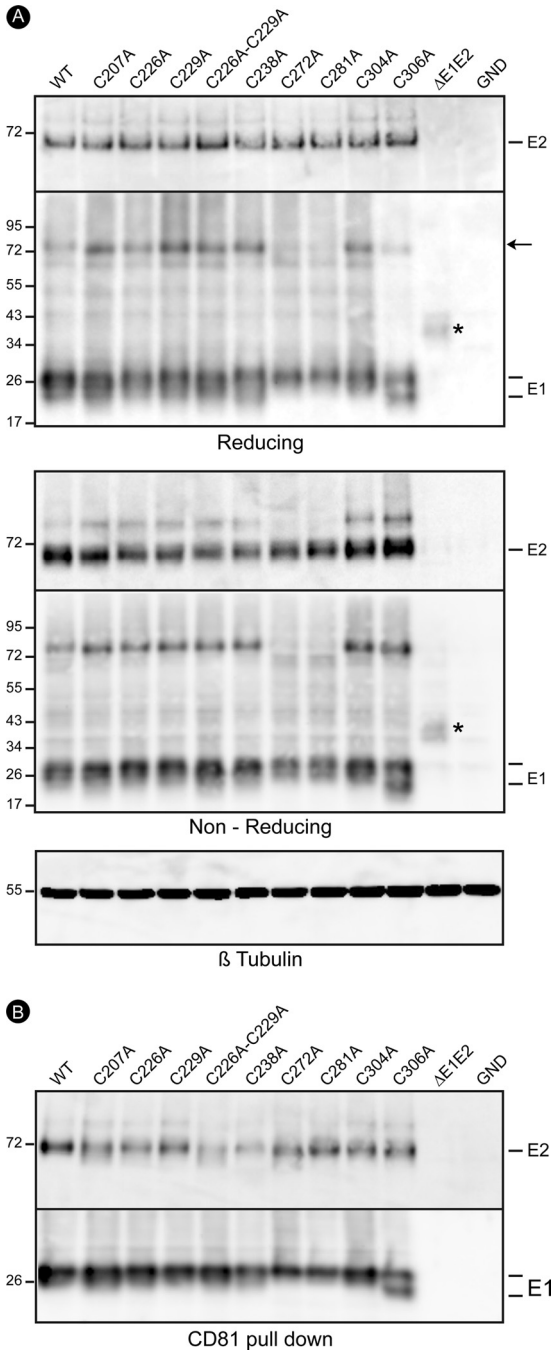


**FIG 5** Mutations of cysteine residues in E1 do not affect E1E2 heterodimerization. (A) Western blotting of HCV envelope glycoproteins. Huh-7 cells were electroporated with E1 mutant viral RNA. At 72 h postelectroporation, the cells were lysed and the proteins were separated by SDS-PAGE and analyzed by Western blotting with MAbs A4 (anti-E1) and 3/11 (anti-E2). Shown are the reducing (top) and nonreducing (bottom) E1 and E2 protein migration profiles. The additional slowly migrating band detected by the anti-E1 antibody under reducing conditions (arrow) likely corresponds to E1 trimers, as previously observed (6). The asterisk corresponds to a small remaining part of E1 protein in the truncated ΔE1E2 virus. Also shown is the beta-tubulin content, which was analyzed to verify that equal amounts of cell lysates had been loaded. (B) Interaction of viral envelope glycoproteins with HCV entry factor CD81. Glutathione-Sepharose beads were incubated with a recombinant form of hCD81 protein LEL in fusion with a GST protein. Pulled-down E1 and E2 proteins were eluted from the beads in Laemmli buffer, analyzed by SDS-PAGE, and revealed by Western blotting with MAbs A4 and 3/11. Molecular mass markers (in kDa) are indicated at the left.

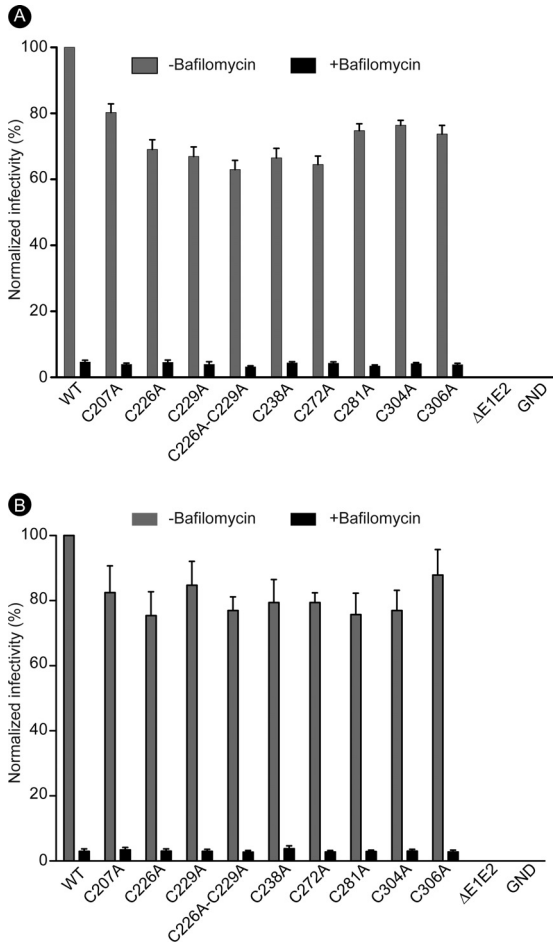


**FIG 6** E1 cysteine mutants do not overcome cell entry blockade induced by bafilomycin A1 at acidic pH. Huh-7 cells were pretreated with bafilomycin A1 (25 nM) (black bars) or not treated (gray bars) and then infected with E1 cysteine mutants along with the WT JFH1 at 4°C for 2 h. The cells were washed to remove unbound virus and then washed with citric acid buffer, pH 7 (A) or pH 5 (B), for 5 min at 37°C. Infected cells were further incubated in the presence of bafilomycin A1 for 48 h. The cells were then fixed, and infected cells were counted and normalized. The values are the combined data from two independent experiments; the error bars represent SEM.

cell transmission was observed after normalization of the data for each mutant (Fig. 7C). Together, these data indicate that E1 cysteine mutants show a decrease in direct cell-to-cell transmission.

**Cysteine mutants in E1 are more sensitive to inhibition by soluble CD81.** Although we did not detect measurable effects of E1 cysteine mutations on the formation of E1E2 heterodimer in HCV-infected cells, we could not exclude more subtle effects on the tridimensional structure of the glycoprotein complex present on the surface of the viral particle. However, due to low infectious titers, a biochemical characterization of the envelope glycoproteins associated with the virions was not possible for E1 cysteine mutants. As an alternative approach, we used a functional assay based on the sensitivity of HCV to entry inhibition by soluble CD81-LEL. As shown in Fig. 8, all E1 cysteine mutants were more sensitive to inhibition with CD81-LEL. Indeed, for most viruses, the mutations led to more than 10-fold reduction of the effective concentration required for half-maximal inhibition ($EC_{50}$) (Table 2). The most sensitive mutants were C229A, C226A-C229A, and

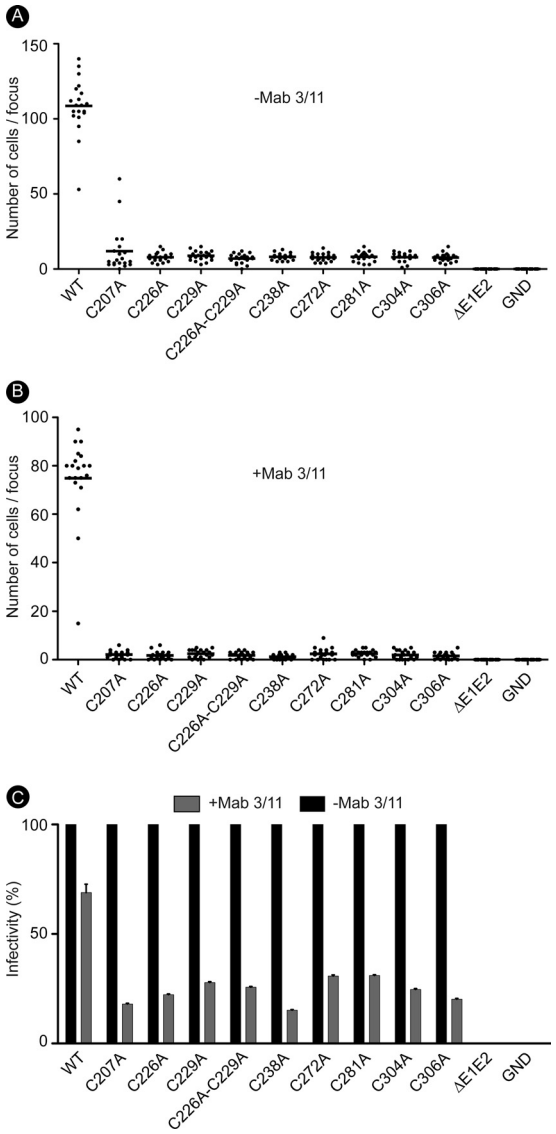


**FIG 7** E1 cysteine mutants show a defect in direct cell-to-cell transmission. (A and B) Huh-7 cells (60,000) were seeded in 24-well plates; the next day, 1,000 infected Huh7.5 RFP-NLS-IPS cells were cocultured in each well. The cultures were treated with 10 μg/ml of MAb 3/11 (B) or not treated (A). The cells were fixed with PFA for 72 h. HCV-infected acceptor cells were visualized with the anti-NS5A monoclonal antibody 9E10 in combination with Alexa Fluor 488-conjugated donkey anti-sheep antibody. The values are the combined data from two independent experiments. Each symbol represents the value for an individual focus, and the short horizontal lines indicate the average number of cells per infected focus. Twenty foci were analyzed per condition. (C) Same as panels A and B, but the number of positive cells for each mutant with the neutralizing 3/11 antibody was normalized to the corresponding value without 3/11 antibody. The error bars represent SEM.

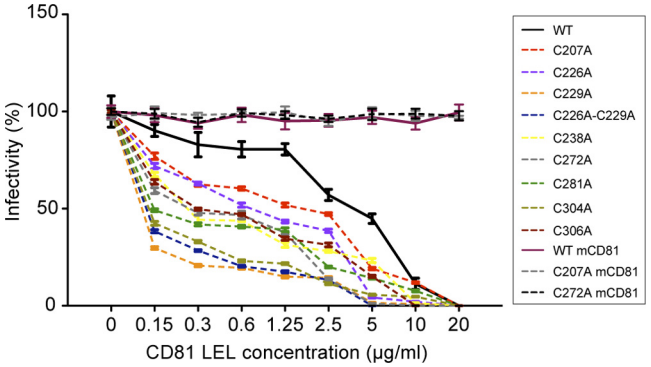


**FIG 8** Cysteine mutants in E1 are more sensitive to inhibition by soluble CD81. Inhibition experiments were performed by incubating E1 mutants or WT virus with various concentrations of human CD81-LEL (0 to 20 μg/ml). After a 2-h incubation period at 37°C, the mixtures were put into contact with target cells for 3 h. After 3 h of contact with virus, the cells were further incubated for 72 h with complete medium. The cells were then immunolabeled, and infected cells were counted. Control experiments were conducted using murine CD81-LEL (mCD81) to investigate its effect on two selected mutants (C207A and C272A) versus human CD81. The data were fitted to the most appropriate linear regression model ($R^2$ = 0.99). The concentrations resulting in 50% inhibition were then determined. The values are the combined data from two independent experiments; the error bars represent SEM.

C304A, with $EC_{50}$s 23.5, 21, and 20 times lower than that of the WT, respectively. The less sensitive mutants were C207A and C226A, for which the $EC_{50}$s were 1.7 and 5.9 times lower than that of the WT, respectively. Together, these results indicate that cysteine mutations in E1 indirectly improve binding to CD81, although the mechanism is still not clear.

**Cysteine mutations in E1 can affect the density of infectious viral particles.** HCV is known to associate with lipoproteins, and this interaction is important for infectivity (reviewed in reference 56). A classical way to measure this interplay is to analyze the sedimentation of infectious viral particles on a density gradient (57, 58). To assess whether E1 cysteine mutations modulate the relationship of HCV with lipoproteins, we compared the buoyant densities of WT virus and some of our mutants. Due to the low level of infectivity of the mutants and their lower stability, we focused our study on two of them. We chose a mutant with a mutation of a cysteine residue located in a hydrophilic region (C207A) and a second mutant with a mutation of a cysteine residue located in a hydrophobic region (C272A) (Fig. 1). In line with previous reports (31), infectivity peaked in a wide range of densities between 1.0 and 1.1 g/ml (Fig. 9A and B). In contrast, infectivity shifted toward higher densities, with a single peak around 1.1 and 1.15 g/ml for the C272A and C207A mutants, respectively. To determine whether these changes can affect the amount of ApoE associated with HCV particles, we tested the sensitivity of C207A and C272A mutants to neutralization by anti-ApoE antibodies. As shown in Fig. 9C, the two mutants showed the same

**TABLE 2** CD81-LEL-GST concentrations resulting in 50% inhibition of virus entry

| Strain | $EC_{50}$ (μg/ml) | SEM | Fold increase in sensitivity to inhibition by CD81-LEL |
|---|---|---|---|
| WT | 4 | 0.61 | |
| C207A | 2.33 | 0.13 | 1.7 |
| C226A | 0.68 | 0.03 | 5.9 |
| C229A | 0.17 | 0.01 | 23.5 |
| C226A-C229A | 0.19 | 0.01 | 21.1 |
| C238A | 0.31 | 0.02 | 12.9 |
| C272A | 0.27 | 0.01 | 14.8 |
| C281A | 0.33 | 0.01 | 12.1 |
| C304A | 0.20 | 0.01 | 20 |
| C306A | 0.38 | 0.01 | 10.5 |

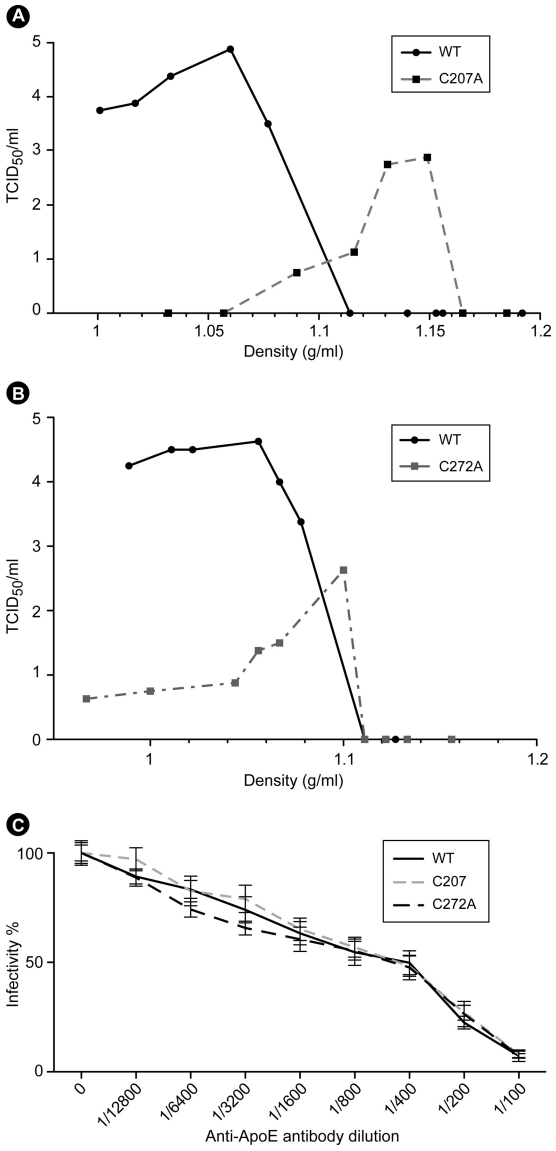


**FIG 9** Cysteine mutations C207A and C272A increase the density of infectious viral particles. (A and B) Separation of concentrated virus in an iodixanol gradient. Concentrated cell-cultured HCV from WT and E1 mutants C207A (A) and C272A (B) were separated by sedimentation through a 10 to 50% iodixanol gradient. Fractions were collected from the top and analyzed for their density, as well as infectivity, by $TCID_{50}$. (C) Effect of anti-ApoE antibody on the neutralization of cysteine mutants. Viruses were incubated with various dilutions of anti-ApoE antibody. After a 2-h incubation period at 37°C, the mixtures were put into contact with target cells. After 3 h of contact with the virus, the cells were further incubated for 72 h with complete medium. The cells were then immunolabeled, and infected cells were counted. The results from two independent experiments are presented as the mean percent infectivity in comparison to a nontreated control; the error bars represent SEM.

sensitivity to anti-ApoE neutralization as the wild-type virus. Together, these data indicate that cysteine mutations in E1 can affect the density of infectious viral particles without necessarily affecting their content in ApoE.

## DISCUSSION

Envelope glycoproteins are essential components of an enveloped viral particle. Indeed, they participate in virus morphogenesis and, by interacting with a cell surface receptor(s) and inducing fusion between the viral envelope and a cellular membrane, they also play an essential role in virus entry into host cells. These multiple functions are associated with dramatic conformational changes that need to be tightly controlled in order to occur at the appropriate location and time. Disulfide bonds are key structural elements for the folding and functions of viral envelope proteins (12, 16). Typically, deletion of disulfide bonds in HCV glycoprotein E2 is indeed deleterious for folding stability and/or production of infectious viral particles. Here, we mutated conserved cysteine residues to investigate the role of disulfide bond formation in HCV glycoprotein E1. Together with E2, this protein forms a functional complex that plays a major role in HCV entry and assembly. Our results show that E1 disulfide bonds are not essential for the production of infectious virus. However, these mutations decreased the efficiency of virus assembly and the stability of the virion. They could also affect the density of infectious viral particles. Furthermore, our results indicate that disulfide bonds in E1 modulate the sensitivity of the virion to inhibition by a soluble form of CD81. Together, these data indicated that E1 stabilizes the structure of E2 on the surface of the HCV particle in order to optimize its assembly and entry functions.

Our mutagenesis experiments identify a new function in E1 glycoprotein, which consists of modulating the entry function of E2. This indicates that cysteine mutations in E1 indirectly modulate E2 glycoprotein functions. Within the HCV glycoprotein heterodimer, E2 is the receptor-binding subunit (reviewed in reference 7) and also likely the fusion protein (5, 59). In contrast, the role of the E1 subunit in HCV entry remains ill defined. However, E1 has also been shown to play a role in the fusion process (8, 9, 10). HCV has been proposed to contain a class II fusion protein (5). In class II viruses, the first glycoprotein acts as a chaperone for the folding of the second one, which carries the membrane fusion function (4). In line with this model, HCV glycoprotein E1 corresponds to the companion chaperone protein, which has been confirmed experimentally (39). However, in the case of HCV, the putative fusion protein, E2, also play a role in the folding stability of the companion protein, E1 (17, 60), indicating a very close interplay between these two proteins during their biogenesis. Furthermore, in contrast to flaviviruses and alphaviruses (14), there is no cleavage of the companion during maturation of the viral particle (6, 61), suggesting that this protein could also be involved in virus entry. It has also been shown that E1 provides some help in the fusion process of HCV particles (8, 9, 10). Here, we show that the companion protein E1 can also affect E2 by potentially modulating its capacity for binding to CD81 coreceptor, although the mechanism is still not clear. Therefore, our data identify additional functions of the companion protein in a class II virus.

Disulfide bonds in HCV envelope glycoprotein E1 are not essential for virus infectivity. Indeed, even if they show a decrease in infectivity, all E1 cysteine mutants are infectious. This is particularly surprising since, due to their covalent nature, disulfide bonds usually play a major role in the folding pathway and the stability of a protein exported in the extracellular milieu. Disulfide bonds can stabilize a protein by reducing the entropy of the unfolded state (62). Furthermore, they can also facilitate the path to the native state if they link parts of a protein that must come into contact early during a folding reaction and can make unfolding less likely if they occur in particularly labile parts of a protein (62). Lack of particular disulfide bonds often affects the structure and functions

of newly synthesized proteins in the ER. Indeed, they either aggregate and fail to fold or they partially oxidize into species similar to folding intermediates of the wild-type protein (63). Since the conformations of viral envelope glycoproteins change at different steps of the viral life cycle, disulfide bonds within these proteins are particularly important to keep them functional. Indeed, mutagenesis of cysteine residues strongly impairs the functions of HCV envelope glycoprotein E2 (12) and HIV envelope glycoprotein (16). Furthermore, in the case of influenza virus hemagglutinin, all disulfide bonds have been reported to be necessary for the protein to reach the native state (16). The conservation of infectivity for E1 cysteine mutants, as also observed for another *Flaviviridae* virus, the pestivirus classical swine fever virus (64), suggests a tolerance for the lack of a disulfide bond within the protein. When expressed alone, E1 has a high tendency to form large aggregates stabilized by disulfide bonds (17), suggesting that the protein would not be tolerant of disruption of disulfide bonds. The rather good tolerance for cysteine mutations in E1 is very likely due to the costabilization role of E2 (17). In the context of the E1E2 heterodimer, E2 stabilizes E1 folding, and disulfide bonds, which form slowly (11), might not be essential for E1 folding. Rather, they could contribute to the stability of the protein in the context of the HCV particle, as discussed below.

Cysteine mutations in E1 affect the assembly of viral particles. Indeed, the quantity of core protein released from electroporated cells decreased drastically compared to the WT, paralleling the decrease in infectivity, which is not due to a defect in secretion, as determined by measuring intracellular infectivity. Virion-associated E1 and E2 envelope glycoproteins form large covalent complexes stabilized by disulfide bonds (6). The presence of disulfide bonds between HCV envelope glycoproteins suggests that lateral protein-protein interactions assisted by disulfide bond formation might play an active role in the budding process of HCV particles. Therefore, disruption of some cysteine residues in E1 might affect these covalent interactions, which could affect virion assembly. Furthermore, the decrease in stability of HCV particles observed for E1 cysteine mutants is likely due to suboptimal intermolecular disulfide bond formation, which can lead to some decrease in virion stability. However, these alterations do not facilitate fusion between the viral particle and the plasma membrane under acidic conditions. Indeed, none of the E1 cysteine mutants could overcome cell entry blockade induced by bafilomycin A1 at acidic pH.

Cysteine mutations in E1 can affect the density of infectious viral particles. Using C207A and C272A mutants, we found that a single cysteine mutation in E1 can cause a shift in the density of infectious HCV particles from a range of 1.0 to 1.1 g/ml to a single peak at approximately 1.1 to 1.15 g/ml. HCV is known to associate with lipoproteins, which explains the relatively heterogeneous and low density of HCV particles (reviewed in reference 56). Changes in virion density have been observed for viruses lacking hypervariable region 1 or showing a single mutation at E2 amino acid position 451 (65, 66, 67). Here, we show that a single mutation in E1 can also similarly affect the density of the viral particle. This observation is in line with the strong interconnection between E1 and E2 subunits, as discussed above. However, it remains unclear how HCV actually associates with lipoproteins. Together with previously reported mutations in E2 (65, 66, 67), our observation that a single mutation in E1 increases the density of HCV particles suggests that the HCV glycoprotein heterodimer influences the interplay between the HCV virion and lipids or lipoproteins. However, further experimental work is needed to better understand the interconnection between HCV glycoprotein heterodimer conformation and virion density.

In conclusion, we show that disulfide bonds are not essential for the entry function of the class II companion glycoprotein E1 of HCV. Rather, they contribute to the stability of the HCV envelope glycoprotein complex at the surface of the virion. Furthermore, our data identify additional functions of a class II companion protein as a molecule that can control the binding capacity of the fusion protein.

## ACKNOWLEDGMENTS

This work was supported by the French National Agency for Research on AIDS and Viral Hepatitis (ANRS) (AO2011-1 CSS4 to J.D.). A.W. was supported by a fellowship from the ANRS.

We are grateful to Sandrine Belouzard and Yves Rouillé for their scientific advice and to Claire Montpellier for her technical help. We are grateful to Sophana Ung for his assistance with the illustrations. We also thank M. Harris, J. McKeating, C. M. Rice, and T. Wakita for providing us with reagents. The fluorescence microscopy data were generated with the help of the Bioimaging Center Lille Nord-de-France (BICeL).

## REFERENCES

1. **Lavanchy D.** 2011. Evolving epidemiology of hepatitis C virus. Clin. Microbiol. Infect. **17**:107–115.
2. **Moradpour D, Penin F, Rice CM.** 2007. Replication of hepatitis C virus. Nat. Rev. Microbiol. **5**:453–463.
3. **Lavie M, Goffard A, Dubuisson J.** 2007. Assembly of a functional HCV glycoprotein heterodimer. Curr. Issues Mol. Biol. **9**:71–86.
4. **Vaney MC, Rey FA.** 2011. Class II enveloped viruses. Cell. Microbiol. **13**:1451–1459.
5. **Krey T, d'Alayer J, Kikuti CM, Saulnier A, Damier-Piolle L, Petitpas I, Johansson DX, Tawar RG, Baron B, Robert B, England P, Persson MA, Martin A, Rey FA.** 2010. The disulfide bonds in glycoprotein E2 of hepatitis C virus reveal the tertiary organization of the molecule. PLoS Pathog. **6**:e1000762. doi:10.1371/journal.ppat.1000762.
6. **Vieyres G, Thomas X, Descamps V, Duverlie G, Patel AH, Dubuisson J.** 2010. Characterization of the envelope glycoproteins associated with infectious hepatitis C virus. J. Virol. **84**:10159–10168.
7. **Dubuisson J, Helle F, Cocquerel L.** 2008. Early steps of the hepatitis C virus life cycle. Cell. Microbiol. **10**:821–827.
8. **Ciczora Y, Callens N, Penin F, Pecheur EI, Dubuisson J.** 2007. Transmembrane domains of hepatitis C virus envelope glycoproteins: residues involved in E1E2 heterodimerization and involvement of these domains in virus entry. J. Virol. **81**:2372–2381.
9. **Drummer HE, Boo I, Poumbourios P.** 2007. Mutagenesis of a conserved fusion peptide-like motif and membrane-proximal heptad-repeat region of hepatitis C virus glycoprotein E1. J. Gen. Virol. **88**:1144–1148.
10. **Lavillette D, Pecheur EI, Donot P, Fresquet J, Molle J, Corbau R, Dreux M, Penin F, Cosset FL.** 2007. Characterization of fusion determinants points to the involvement of three discrete regions of both E1 and E2 glycoproteins in the membrane fusion process of hepatitis C virus. J. Virol. **81**:8752–8765.
11. **Dubuisson J, Rice CM.** 1996. Hepatitis C virus glycoprotein folding: disulfide bond formation and association with calnexin. J. Virol. **70**:778–786.
12. **McCaffrey K, Boo I, Tewierek K, Edmunds ML, Poumbourios P, Drummer H.** 2012. Role of conserved cysteine residues in hepatitis C virus glycoprotein e2 folding and function. J. Virol. **86**:3961–3974.
13. **Ellgaard L, Helenius A.** 2003. Quality control in the endoplasmic reticulum. Nat. Rev. Mol. Cell Biol. **4**:181–191.
14. **Kielian M, Rey FA.** 2006. Virus membrane-fusion proteins: more than one way to make a hairpin. Nat. Rev. Microbiol. **4**:67–76.
15. **McCaffrey K, Boo I, Poumbourios P, Drummer HE.** 2007. Expression and characterization of a minimal hepatitis C virus glycoprotein E2 core domain that retains CD81 binding. J. Virol. **81**:9584–9590.
16. **van Anken E, Sanders RW, Liscaljet IM, Land A, Bontjer I, Tillemans S, Nabatov AA, Paxton WA, Berkhout B, Braakman I.** 2008. Only five of 10 strictly conserved disulfide bonds are essential for folding and eight for

function of the HIV-1 envelope glycoprotein. Mol. Biol. Cell **19**:4298–4309.
17. **Michalak J-P, Wychowski C, Choukhi A, Meunier J-C, Ung S, Rice CM, Dubuisson J.** 1997. Characterization of truncated forms of hepatitis C virus glycoproteins. J. Gen. Virol. **78**:2299–2306.
18. **Combet C, Garnier N, Charavay C, Grando D, Crisan D, Lopez J, Dehne-Garcia A, Geourjon C, Bettler E, Hulo C, Le Mercier P, Bartenschlager R, Diepolder H, Moradpour D, Pawlotsky JM, Rice CM, Trepo C, Penin F, Deleage G.** 2007. euHCVdb: the European hepatitis C virus database. Nucleic Acids Res. **35**:D363–D366.
19. **Combet C, Blanchet C, Geourjon C, Deleage G.** 2000. NPS@: network protein sequence analysis. Trends Biochem. Sci. **25**:147–150.
20. **Thompson JD, Higgins DG, Gibson TJ.** 1994. CLUSTAL W: improving the sensitivity of progressive multiple sequence alignment through sequence weighting, position-specific gap penalties and weight matrix choice. Nucleic Acids Res. **22**:4673–4680.
21. **Cserzo M, Wallin E, Simon I, von Heijne G, Elofsson A.** 1997. Prediction of transmembrane alpha-helices in procariotic membrane proteins: the Dense Alignment Surface method. Protein Eng. **10**:673–676.
22. **Tusnady GE, Simon I.** 1998. Principles governing amino acid composition of integral membrane proteins: application to topology prediction. J. Mol. Biol. **283**:489–506.
23. **Hofmann K, Stoffel W.** 1993. A database of membrane spanning protein segments. Biol. Chem. Hoppe-Seyler **374**:166.
24. **Krogh A, Larsson B, von Heijne G, Sonnhammer EL.** 2001. Predicting transmembrane protein topology with a hidden Markov model: application to complete genomes. J. Mol. Biol. **305**:567–580.
25. **Claros MG, von Heijne G.** 1994. TopPred II: an improved software for membrane protein structure predictions. Comput. Appl. Biosci. **10**:685–686.
26. **Hirokawa T, Boon-Chieng S, Mitaku S.** 1998. SOSUI: classification and secondary structure prediction system for membrane proteins. Bioinformatics **14**:378–379.
27. **Jones CT, Catanese MT, Law LM, Khetani SR, Syder AJ, Ploss A, Oh TS, Schoggins JW, MacDonald MR, Bhatia SN, Rice CM.** 2010. Real-time imaging of hepatitis C virus infection using a fluorescent cell-based reporter system. Nat. Biotechnol. **28**:167–171.
28. **Nakabayashi H, Taketa K, Miyano K, Yamane T, Sato J.** 1982. Growth of human hepatoma cells lines with differentiated functions in chemically defined medium. Cancer Res. **42**:3858–3863.
29. **Dubuisson J, Hsu HH, Cheung RC, Greenberg HB, Russell DG, Rice CM.** 1994. Formation and intracellular localization of hepatitis C virus envelope glycoprotein complexes expressed by recombinant vaccinia and Sindbis viruses. J. Virol. **68**:6147–6160.
30. **Flint M, Maidens C, Loomis-Price LD, Shotton C, Dubuisson J, Monk P, Higginbottom A, Levy S, McKeating JA.** 1999. Characterization of hepatitis C virus E2 glycoprotein interaction with a putative cellular receptor, CD81. J. Virol. **73**:6235–6244.
31. **Lindenbach BD, Evans MJ, Syder AJ, Wolk B, Tellinghuisen TL, Liu CC, Maruyama T, Hynes RO, Burton D, McKeating JA, Rice CM.** 2005. Complete replication of hepatitis C virus in cell culture. Science **309**:623–626.
32. **Wakita T, Pietschmann T, Kato T, Date T, Miyamoto M, Zhao Z, Murthy K, Habermann A, Krausslich HG, Mizokami M, Bartenschlager R, Liang TJ.** 2005. Production of infectious hepatitis C virus in tissue culture from a cloned viral genome. Nat. Med. **11**:791–796.
33. **Delgrange D, Pillez A, Castelain S, Cocquerel L, Rouillé Y, Dubuisson J, Wakita T, Duverlie G, Wychowski C.** 2007. Robust production of infectious viral particles in Huh-7 cells by introducing mutations in hepatitis C virus structural proteins. J. Gen. Virol. **88**:2495–2503.
34. **Goueslain L, Alsaleh K, Horellou P, Roingeard P, Descamps V, Duverlie G, Ciczora Y, Wychowski C, Dubuisson J, Rouillé Y.** 2010. Identification of GBF1 as a cellular factor required for hepatitis C virus RNA replication. J. Virol. **84**:773–787.
35. **Mederacke I, Wedemeyer H, Ciesek S, Steinmann E, Raupach R, Wursthorn K, Manns MP, Tillmann HL.** 2009. Performance and clinical utility of a novel fully automated quantitative HCV-core antigen assay. J. Clin. Virol. **46**:210–215.
36. **Morota K, Fujinami R, Kinukawa H, Machida T, Ohno K, Saegusa H, Takeda K.** 2009. A new sensitive and automated chemiluminescent microparticle immunoassay for quantitative determination of hepatitis C virus core antigen. J. Virol. Methods **157**:8–14.
37. **Higginbottom A, Quinn ER, Kuo CC, Flint M, Wilson LH, Bianchi E, Nicosia A, Monk PN, McKeating JA, Levy S.** 2000. Identification of amino acid residues in CD81 critical for interaction with hepatitis C virus envelope glycoprotein E2. J. Virol. **74**:3642–3649.
38. **Meuleman P, Albecka A, Belouzard S, Vercauteren K, Verhoye L, Wychowski C, Leroux-Roels G, Palmer KE, Dubuisson J.** 2011. Griffithsin has antiviral activity against hepatitis C virus. Antimicrob. Agents Chemother. **55**:5159–5167.
39. **Brazzoli M, Helenius A, Foung SK, Houghton M, Abrignani S, Merola M.** 2005. Folding and dimerization of hepatitis C virus E1 and E2 glycoproteins in stably transfected CHO cells. Virology **332**:438–453.
40. **Deleersnyder V, Pillez A, Wychowski C, Blight K, Xu J, Hahn YS, Rice CM, Dubuisson J.** 1997. Formation of native hepatitis C virus glycoprotein complexes. J. Virol. **71**:697–704.
41. **Merola M, Brazzoli M, Cocchiarella F, Heile JM, Helenius A, Weiner AJ, Houghton M, Abrignani S.** 2001. Folding of hepatitis C virus E1 glycoprotein in a cell-free system. J. Virol. **75**:11205–11217.
42. **Kuiken C, Mizokami M, Deleage G, Yusim K, Penin F, Shin IT, Charavay C, Tao N, Crisan D, Grando D, Dalwani A, Geourjon C, Agrawal A, Combet C.** 2006. Hepatitis C databases, principles and utility to researchers. Hepatology **43**:1157–1165.
43. **Op De Beeck A, Montserret R, Duvet S, Cocquerel L, Cacan R, Barberot B, Le Maire M, Penin F, Dubuisson J.** 2000. Role of the transmembrane domains of hepatitis C virus envelope proteins E1 and E2 in the assembly of the noncovalent E1E2 heterodimer. J. Biol. Chem. **275**:31428–31437.
44. **Schlessinger A, Yachdav G, Rost B.** 2006. PROFbval: predict flexible and rigid residues in proteins. Bioinformatics **22**:891–893.
45. **Spadaccini R, D'Errico G, D'Alessio V, Notomista E, Bianchi A, Merola M, Picorne D.** 2010. Structural characterization of the transmembrane proximal region of the hepatitis C virus E1 glycoprotein. Biochim. Biophys. Acta **1798**:344–353.
46. **Perez-Berna AJ, Pabst G, Laggner P, Villalain J.** 2009. Biophysical characterization of the fusogenic region of HCV envelope glycoprotein E1. Biochim. Biophys. Acta **1788**:2183–2193.
47. **Gastaminza P, Kapadia SB, Chisari FV.** 2006. Differential biophysical properties of infectious intracellular and secreted hepatitis C virus particles. J. Virol. **80**:11074–11081.
48. **Cocquerel L, Quinn ER, Flint M, Hadlock KG, Foung SK, Levy S.** 2003. Recognition of native hepatitis C virus E1E2 heterodimers by a human monoclonal antibody. J. Virol. **77**:1604–1609.
49. **Pileri P, Uematsu Y, Campagnoli S, Galli G, Falugi F, Petracca R, Weiner AJ, Houghton M, Rosa D, Grandi G, Abrignani S.** 1998. Binding of hepatitis C virus to CD81. Science **282**:938–941.
50. **Petracca R, Falugi F, Galli G, Norais N, Rosa D, Campagnoli S, Burgio V, Di Stasio E, Giadina B, Houghton M, Abrignani S, Grandi G.** 2000. Structure-function analysis of hepatitis C virus envelope-CD81 binding. J. Virol. **74**:4824–4830.
51. **Blanchard E, Belouzard S, Goueslain L, Wakita T, Dubuisson J, Wychowski C, RouillÉ Y.** 2006. Hepatitis C virus entry depends on clathrin-mediated endocytosis. J. Virol. **80**:6964–6972.
52. **Tscherne DM, Jones CT, Evans MJ, Lindenbach BD, McKeating JA, Rice CM.** 2006. Time- and temperature-dependent activation of hepatitis C virus for low-pH-triggered entry. J. Virol. **80**:1734–1741.
53. **Timpe JM, Stamataki Z, Jennings A, Hu K, Farquhar MJ, Harris HJ, Schwarz A, Desombere I, Leroux-Roels G, Balfe P, McKeating JA.** 2008. Hepatitis C virus cell-cell transmission in hepatoma cells in the presence of neutralizing antibodies. Hepatology **47**:17–24.
54. **Witteveldt J, Evans MJ, Bitzegeio J, Koutsoudakis G, Owsianka AM, Angus AG, Keck ZY, Foung SK, Pietschmann T, Rice CM, Patel AH.** 2009. CD81 is dispensable for hepatitis C virus cell-to-cell transmission in hepatoma cells. J. Gen. Virol. **90**:48–58.
55. **Brimacombe CL, Grove J, Meredith LW, Hu K, Syder AJ, Flores MV, Timpe JM, Krieger SE, Baumert TF, Tellinghuisen TL, Wong-Staal F, Balfe P, McKeating JA.** 2011. Neutralizing antibody-resistant hepatitis C virus cell-to-cell transmission. J. Virol. **85**:596–605.
56. **Bartenschlager R, Penin F, Lohmann V, Andre P.** 2011. Assembly of infectious hepatitis C virus particles. Trends Microbiol. **19**:95–103.
57. **Lindenbach BD, Meuleman P, Ploss A, Vanwolleghem T, Syder AJ, McKeating JA, Lanford RE, Feinstone SM, Major M, Leroux-Roels G, Rice CM.** 2006. Cell culture-grown hepatitis C virus is infectious in vivo and can be recultured in vitro. Proc. Natl. Acad. Sci. U. S. A. **103**:3805–3809.
58. **Zhong J, Gastaminza P, Chung J, Stamataki Z, Isogawa M, Cheng G,**

**McKeating JA, Chisari FV.** 2006. Persistent hepatitis C virus infection in vitro: coevolution of virus and host. J. Virol. **80**:11082–11093.
59. **Sharma NR, Mateu G, Dreux M, Grakoui A, Cosset FL, Melikyan GB.** 2011. Hepatitis C virus is primed by CD81 protein for low pH-dependent fusion. J. Biol. Chem. **286**:30361–30376.
60. **Patel J, Patel AH, McLauchlan J.** 2001. The transmembrane domain of the hepatitis C virus E2 glycoprotein is required for correct folding of the E1 glycoprotein and native complex formation. Virology **279**:58–68.
61. **Op De Beeck A, Voisset C, Bartosch B, Ciczora Y, Cocquerel L, Keck Z, Foung S, Cosset FL, Dubuisson J.** 2004. Characterization of functional hepatitis C virus envelope glycoproteins. J. Virol. **78**:2994–3002.
62. **Feige MJ, Hendershot LM.** 2011. Disulfide bonds in ER protein folding and homeostasis. Curr. Opin. Cell Biol. **23**:167–175.
63. **Braakman I, Bulleid NJ.** 2011. Protein folding and modification in the mammalian endoplasmic reticulum. Annu. Rev. Biochem. **80**:71–99.
64. **Fernandez-Sainz I, Holinka LG, Gladue D, O'Donnell V, Lu Z, Gavrilov BK, Risatti GR, Borca MV.** 2011. Substitution of specific cysteine residues in the E1 glycoprotein of classical swine fever virus strain Brescia affects formation of E1-E2 heterodimers and alters virulence in swine. J. Virol. **85**:7264–7272.
65. **Bankwitz D, Steinmann E, Bitzegeio J, Ciesek S, Friesland M, Herrmann E, Zeisel MB, Baumert TF, Keck ZY, Foung SK, Pecheur EI, Pietschmann T.** 2010. Hepatitis C virus hypervariable region 1 modulates receptor interactions, conceals the CD81 binding site, and protects conserved neutralizing epitopes. J. Virol. **84**:5751–5763.
66. **Grove J, Nielsen S, Zhong J, Bassendine MF, Drummer HE, Balfe P, McKeating JA.** 2008. Identification of a residue in hepatitis C virus E2 glycoprotein that determines scavenger receptor BI and CD81 receptor dependency and sensitivity to neutralizing antibodies. J. Virol. **82**:12020–12029.
67. **Prentoe J, Jensen TB, Meuleman P, Serre SB, Scheel TK, Leroux-Roels G, Gottwein JM, Bukh J.** 2011. Hypervariable region 1 differentially impacts viability of hepatitis C virus strains of genotypes 1 to 6 and impairs virus neutralization. J. Virol. **85**:2224–2234.